Diurnal and seasonal patterns of carbon dioxide and its vertical structure in the atmosphere

MORGAN CLARK*

National Weather Center Research Experiences for Undergraduates Program
Norman, Oklahoma

SEAN CROWELL, ELIZABETH A. PILLAR-LITTLE[†], PETRA KLEIN[‡], XIAO-MING HU[§], JEFFERY BASARA, AND PHILLIP B. CHILSON

University of Oklahoma School of Meteorology
Norman, Oklahoma

XIANGMING XIAO

Center for Spatial Analysis
Norman, Oklahoma

ABSTRACT

Understanding carbon dioxide (CO_2) sources and sinks provides us with the information necessary to control the planet's total warming. The planetary boundary layer (PBL) retains a significant amount of emissions. To understand local emissions, it is useful to partition CO_2 emissions between the PBL and free troposphere. This paper analyzes model output data using the weather research and forecasting, vegetation photosynthesis respiration model (WRF-VPRM) and manned aircraft data collected in Lamont, Oklahoma. This analysis studies the vertical gradients of CO_2 in the atmosphere as well as the seasonal and diurnal cycles of emissions. The results are compared to prior studies. The main drivers of CO_2 in the PBL are investigated diurnally as well as for monthly averages.

1. Introduction

Carbon dioxide (CO_2) research is necessary to expand our knowledge and comprehension of our future climate. By understanding sources and sinks of CO_2, one can obtain a better understanding of the biological and anthropogenic contributions to the carbon cycle. By examining changes in the concentration of CO_2, we can learn about the emissions. In particular, partitioning the concentrations between the planetary boundary layer (PBL) and the free troposphere tells us about local emissions. The PBL is defined as the lowest 1-2 km of the atmosphere and is heavily influenced by its interactions with the surface. Its height is dependent on convection (Panofsky 1985). The PBL is the level of the atmosphere in which humans, plants, and animals interact with the environment; therefore, there should be more variable CO_2 concentrations.

The flux is composed of the anthropogenic and biological components, therefore, it is important to know the net ecosystem exchange (NEE) which is the balance of photosynthesis and respiration. (Hilton et al. 2014). NEE controls the magnitude of CO_2 uptake. In this study, NEE is estimated using the vegetation photosynthetic respiration model (VPRM).

It is also important to examine the vertical profiles of CO_2. These profiles contain information on local and regional processes because of strong vertical mixing in the planetary boundary layer and free tropospheric transport (Lan et al. 2017).

Numerous studies have been conducted to understand land-atmosphere coupling (Friedlingstein et al. 2014). These studies use eddy covariance (EC) towers and manned aircraft collection to gather data. Earlier land surface models had trouble with predicting terrestrial sink strengths with a wide variety of flux magnitude and sign by the year 2100 (Friedlingstein et al. 2006). EC towers are sparse and with the improvement of land surface models, comes an improvement of diagnostic skill for fluxes where direct observations do not exist (Hilton et al. 2013).

When comparing observed CO_2, Yi et al. (2004) found the General Circulation Model coupled with the Simple Biosphere model successfully predicted CO_2 concentrations using measurements from an EC tower in a northern Wisconsin forest. A strong seasonal pattern of covariance of PBL heights and CO_2 emissions existed. How-

**Corresponding author address:* The Ohio State University, Columbus, OH
E-mail: clark.2649@buckeyemail.osu.edu

ever, the models used predicted a much shallower PBL, which in turn, underestimated the diurnal covariance. Lan et al. (2017) conducted a study using both EC tower and aircraft measurements. It was discovered that the largest variability occurred in the boundary layer. There was little variance seasonally and spatially in the upper atmosphere (greater than 2 km). The PBL is heavily influenced by surface emissions which causes a deep drawdown in the summertime due to photosynthetic activity.

The following study analyzes the model output from the weather researching and forecasting (WRF) model coupled with a carbon cycle land surface model, Vegetation Photosynthesis Respiration model (VPRM) and compares it to observations from flight collection in Lamont, Oklahoma. By using WRF-VPRM, CO_2 emissions and concentrations can be analyzed in the free troposphere and the boundary layer. Seasonal and diurnal patterns of CO_2 and NEE were analyzed to further investigate its structure in the atmosphere.

2. Methods

2.1 Vegetation Photosynthesis Respiration Model (VPRM)

WRF-Chem is coupled with chemistry which simulates the emission, transport, and interactions of aerosols and gases in the atmosphere with the modeled meteorology. WRF-Chem uses CO_2 biosphere fluxes modeled by the VPRM.

NEE is modeled by VPRM by using a combination of modeled, gross ecosystem exchange (GEE) and an ecosystem respiration component (Hilton et al. 2013). NEE is calculated by

$$NEE = GEE + RES \tag{1}$$

where GEE is the carbon flux from plants to atmosphere due to photosynthesis, and RES is the respiration component.

GEE, the photosynthetic component of the model, is a function of shortwave radiation and surface temperature which are modeled by WRF-Chem. This is a critical component because solar radiation is the driving force for photosynthesis and turbulent convection (Yi et al. 2004). GEE is also influenced by the Moderate Resolution Imaging Spectroradiometer (MODIS) components, land surface water index (LSWI) and enhanced vegetation index (EVI). MODIS-EVI shows the contribution of vegetation properties for reliable comparisons of terrestrial photosynthetic activity and structure variability in the canopy. It is computed without bias or assumptions based on the land cover class, soil type, or climate. EVI is calculated globally over 1 km of land with a 500 m resolution (Huete et al. 2002). GEE can be found by

$$GEE = (\lambda \times T_{scale} \times W_{scale} \times P_{scale}) \times FAPAR_{PAV} \times \frac{1}{(1+\frac{PAR}{PAR_0})} \times PAR$$

where λ is the slope of the light response curve from flux data, T_{scale} is the relationship between photosynthesis and the temperature derived from meteorological data, W_{scale} is the canopy moisture and P_{scale} is the impact of leaf expansion, both from MODIS-LSWI, $FAPAR_{PAV}$ is the fraction of photosynthetically active radiation absorbed by the photosynthetically active portion of vegetation, derived from MODIS-EVI, and PAR and PAR_0 are the photosynthetically active radiation and half saturation value for photosynthesis, respectively, both derived from meteorological data.

The respiration component is a function of WRF-modeled surface temperatures. RES can be found by

$$RES = \alpha \times T + \beta \tag{2}$$

where α and β are constants, β is the minimal respiration that occurs regardless of temperature.

The model captures synoptic events, such as the cold front shown in Fig. 1. The model simulates a relatively low concentration of CO_2 behind the cold front and in front of the warm front. There is also a higher concentration near the warm side of the frontal boundary. The inclusion of synoptic events affecting CO_2 concentrations is integral to the study as it helps us understand the importance of daily influences on CO_2.

2.2 Flight data and site

Flight data was collected regularly from 2006-2016 during the afternoon in Lamont, Oklahoma. Since the model data was only available for 2016, only the data from 2016 was used. Lamont is situated in Southern Great Plains region in northern Oklahoma and is classified as a cropland land cover (Fischer and Lindenmayer 2007). It is not downwind from any major cities and has a low population of 417 according to the 2010 US Census (United States Census cited 2018). The small amount of human activity could help provide a baseline for how CO_2 should move in the atmosphere.

Data was collected in the afternoon as the well-mixed PBL provides the most reasonable CO2 flux measurements (Helliker et al. 2004). The trace CO_2 mole fraction in dry air was collected and recorded along with the height, time, longitude, and latitude.

2.3 Data Analysis

In this study, collected data from the 2016 flights to the modeled CO_2 will be compared. The multi-layer CO_2, average dry air mixing ratio can be calculated by

$$\frac{\sum CO_2^i \Delta P^i}{\sum \Delta P^i} \tag{3}$$

where ΔP^i is the thickness of pressure layer i, CO_2^i is the mixing ratio in layer i, PBL CO_2 is defined as the CO_2

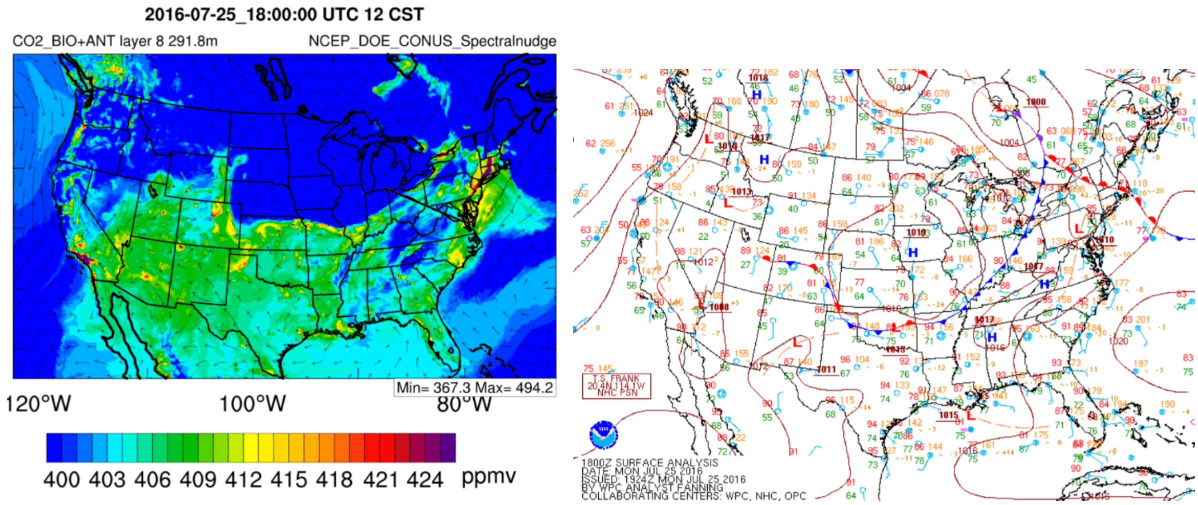

(a) (b)

FIG. 1: Map of the CO_2 concentrations in parts per million (ppm) on July 25th, 2016 at 1800Z (a). Surface map of weather conditions at 1800Z on July 25th, 2016 (b). Clear frontal systems are defined by the concentration gradients (Hu et al. 2018) and (Hu et al. 2018a).

mixing ratio below the PBL, and the free troposphere CO_2 is the CO_2 mixing ratio above the PBL and below 5km. This height is chosen to better match the measurements collected in the Lamont flights that reached a maximum of 5-6 km.

The time series plots of daily and weekly CO_2 and NEE fluxes help identify any anomalies and patterns that differ from the average diurnal pattern. This comparison will show how the CO_2 is affected by NEE flux and how that could impact future data collection. We also analyze the monthly diurnal pattern of NEE to assess its changes by season.

3. Results

3.1 Comparisons of CO2 in the PBL and the Free Troposphere

Comparing the model output of the total biogenic and anthropogenic CO_2 at two layers, 12.1865m and 2785.25m above ground level, obvious differences in CO_2 concentrations are observed. Helliker et al. (2004) suggest that the vertical CO2 gradient between the PBL and free troposphere as well as the gradient between latitudes are larger then what is observed in the free troposphere. This can be seen in Fig. 2a, there are noticeable hot spots of CO_2 concentrated near cities with high populations closer to the surface. This is due to the heavy output of fossil fuels and CO_2 emitted by large populations. This observation is not consistent in the upper level map. In Fig. 2b, these hot spots are absent due to the homogeneous amounts of CO_2 in the upper atmosphere. At 2785m, the effects of human activity are not present in CO_2 concentrations. The effects of high CO_2 concentrations appear to be due to upper level air flow. Air flow is also a large influence in surface layer CO_2 concentrations which is shown in Fig. 2a.

Temporal observations show little variability of CO_2 in the free troposphere as well. The modeled monthly averaged diurnal cycle of CO_2 was plotted, separating both PBL and free troposphere CO_2 from one another. In Fig. 3, CO_2 has more variability throughout the day in the boundary layer rather than the free troposphere. CO_2 concentration tends to be uniform at higher altitudes. The monthly average diurnal pattern of NEE was plotted in Fig. 4 alongside PBL CO_2. There appears to be a delayed response from the NEE onto the PBL CO_2. This suggests that NEE is a driving force for the concentration of CO_2 in the boundary layer, but NEE is greater than zero even though PBL CO_2 is decreasing. This means that the decrease is due to PBL growth.

3.2 Vertical Profiles

The homogeneity in the upper atmosphere can also be seen in flights. In Fig. 5, there is high variability of CO_2 concentration around the modeled PBL. As heights increase, CO_2 approaches the same concentration amongst all flight days.

We compared the vertical profiles of the modeled CO_2 to the modeled PBL depth to determine the vertical gradient of modeled CO_2. By comparing the vertical profiles of

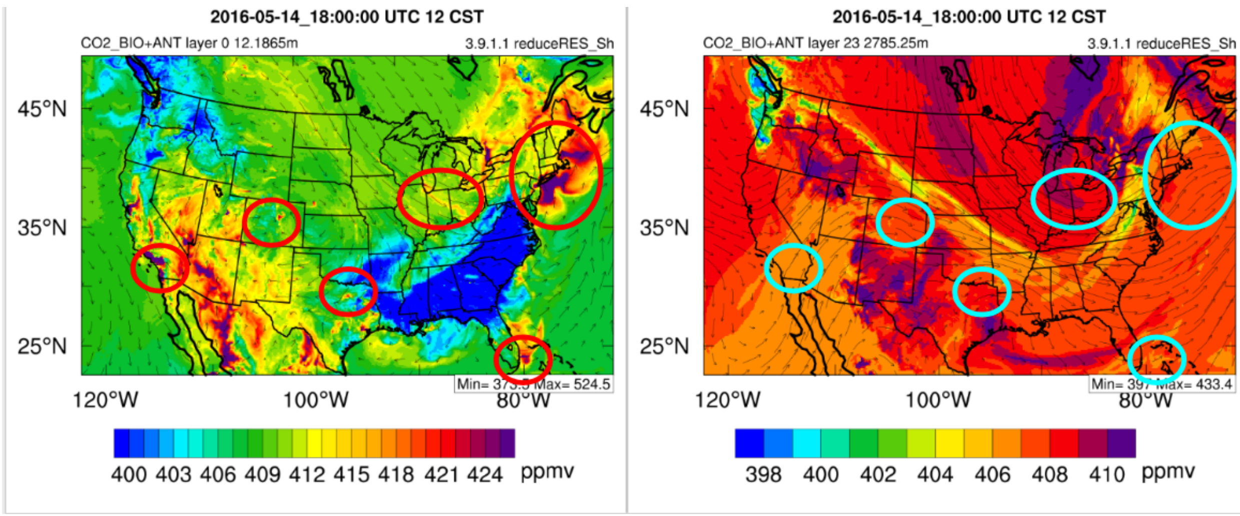

FIG. 2: CO_2 hotspots are seen in large cities near the surface (a) that are not visible in the upper air map (b).

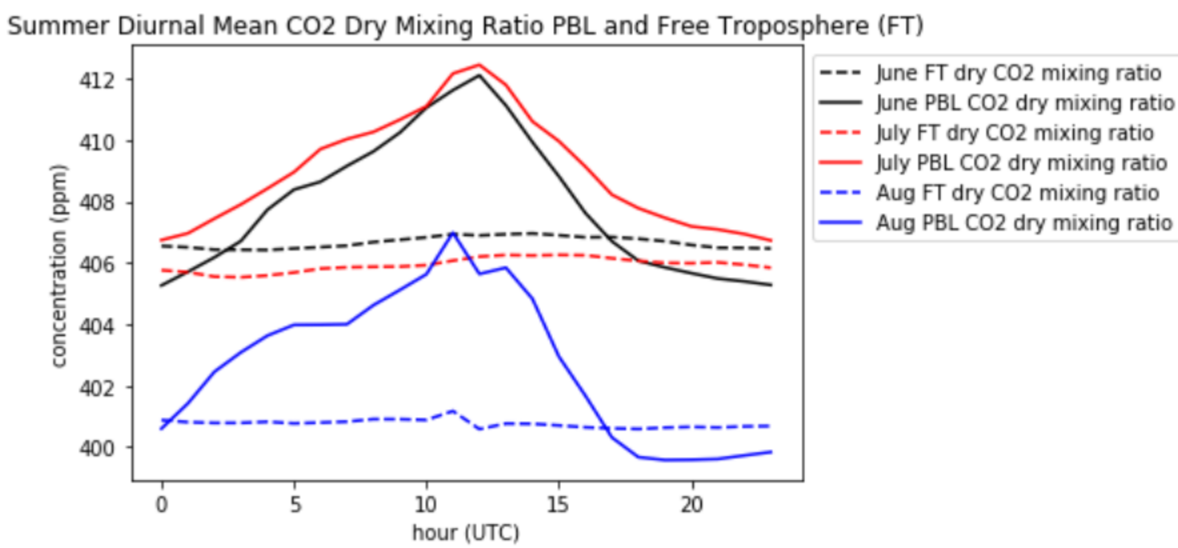

FIG. 3: Mean diurnal CO_2 dry mixing ratios in the boundary layer (PBL) and free troposphere (FT) for June, July, and August.

the flight data to the modeled profiles, we can determine if the shape of the model profile is consistent with real world data. In the model, there is a slight increase in concentration of CO_2 as it reaches the top of the PBL (Figure 6a). This increase typically is shown throughout the PBL and slightly above it. When plotted with the modeled PBL, the vertical profile of the flight data shows changes around the PBL which agrees with the modeled CO_2 profile (Figure 6b).

Independent rawindsonde analysis suggests that the behavior of the aircraft profiles in the PBL and free troposphere is similar to the model profiles, when the actual PBL height is taken into consideration (not shown).

4. Discussion

The delayed drawdown of NEE onto this PBL CO_2 is prominent in monthly averages, but when analyzing the two during a week-long time scale (Figure 7), there is less of a correlation in the summertime. This is possibly due to higher wind speeds in the summer. As one would expect, the positive flux of the NEE should increase the PBL CO_2

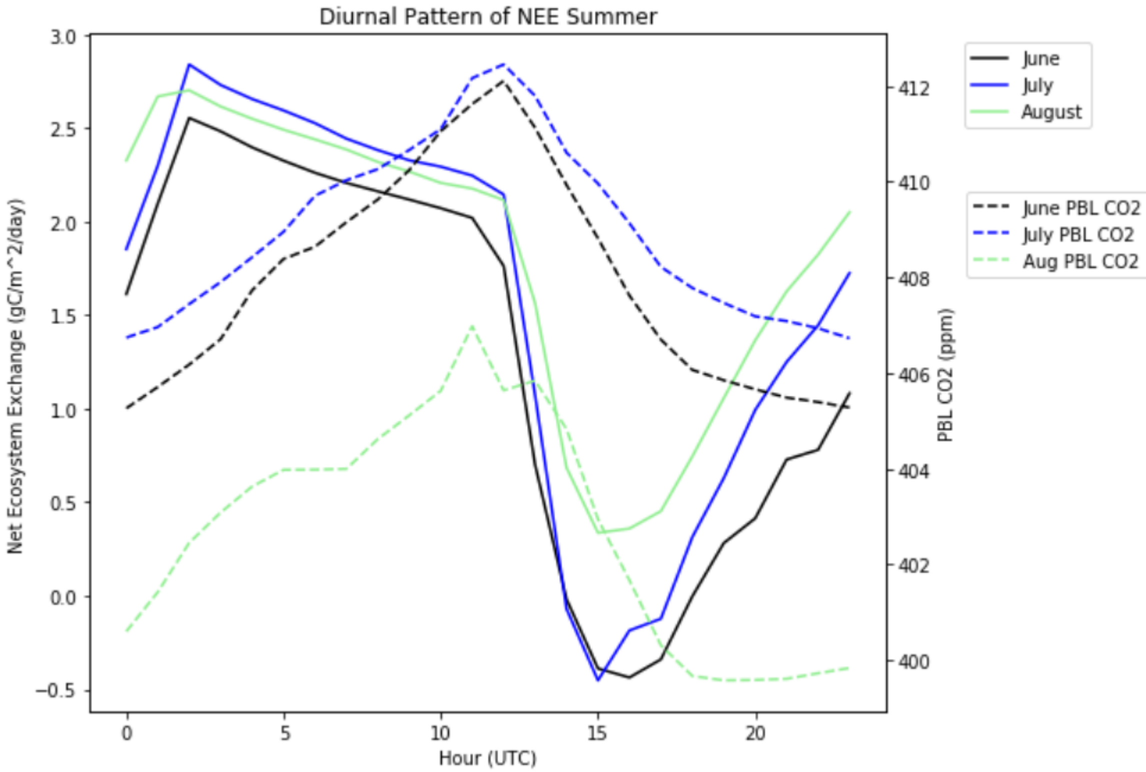

FIG. 4: Comparisons between the CO_2 mixing ratio in the PBL and the net ecosystem exchange (NEE) for June, July, and August.

concentration. However, the deeper PBL depths imply that more dry air dilutes the CO_2 concentrations. The weaker drawdown in the summertime from both the PBL CO_2 and the NEE suggest that the PBL depth dominates the CO_2 concentration in summer.

In the summertime, it is expected for the CO_2 to deplete during the day due to photosynthesis, but this is diluted by the convective mixing in the boundary layer. At night, CO_2 accumulates near the surface due to respiration. This behavior is observed by the model; however, it is also expected for net emissions to be negative in the summer and positive in the winter. This is not in agreement with the model.

In Yi et al. (2004), the largest observed and modeled CO_2 flux is in the autumn. The large positive flux observed by Yi et al. agrees with our results (Figure 8). This was not observed in seasonal NEE. Yi et al found there to be more negative NEE in the summer, our model produced a negative drawdown only in July. This study differed from Yi et al. because their observations were conducted in a Wisconsin forest which has more vegetation than Lamont. After further observations of the respiration and GEE components (Fig. 9), it can be assumed that the small GEE in the summertime causes the positive net flux. This is due to reduced photosynthesis possibly from the MODIS output.

When examining the flight data, there are also clear differences between CO_2 in the free troposphere and the PBL. In future work, it would be beneficial to include multiple years of analysis and samples from other locations. This would provide a better discrimination between the influence of PBL dynamics and surface fluxes on CO_2 measurements.

Another limitation about this location is that it has been known to have a less-pronounced seasonal cycle for CO_2 in comparison to forested regions or regions with more vegetation (Lan et al. 2017). It is seen in Midwestern regions that photosynthesis creates a drawdown in the summertime and respiration is highest in the fall, winter, and summer (Helliker et al. 2004). This differs from our seasonal results and future work could investigate other comparisons.

5. Conclusion

Both the model and flight data suggest that there is little variability in CO_2 concentration above the PBL. There is also a considerable difference in concentration between

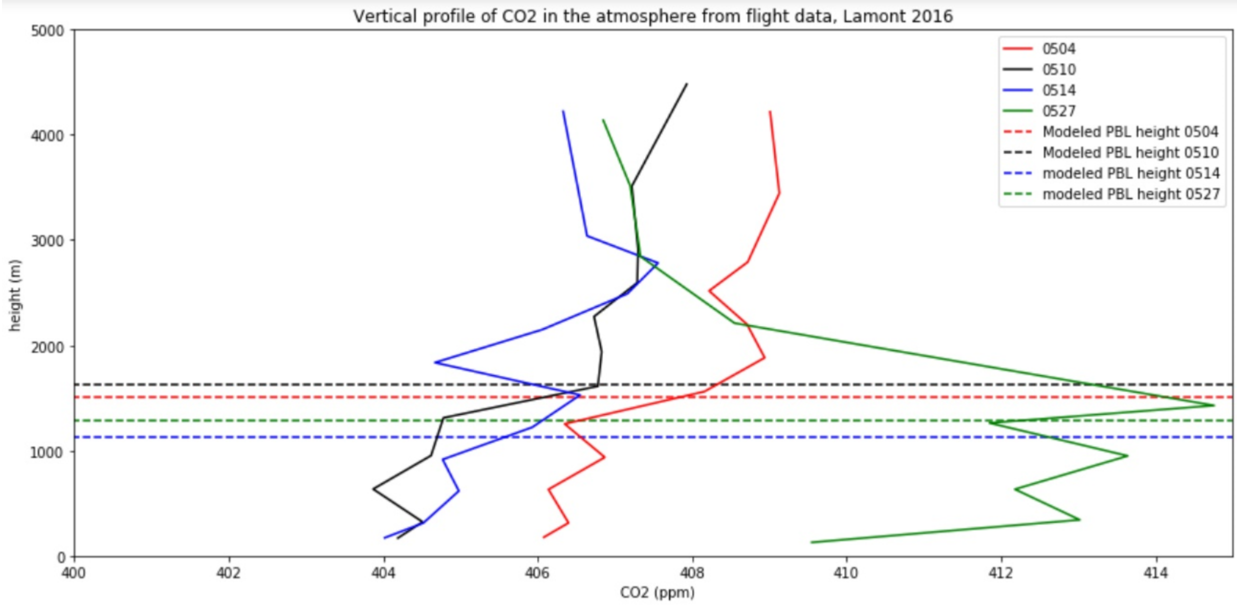

FIG. 5: Vertical profile of CO_2 concentration collected during flights of May 2016

the average dry mixing ratio of CO_2 in the free troposphere and in the PBL. The model shows that NEE is a driver of PBL CO_2 mixing ratio when compared over averaged timescales but can vary in influence daily.

WRF-VPRM agrees with the flight data collected in Lamont by its ability to predict the overall vertical structure of CO_2 concentration in the atmosphere. The flight data in this study was collected in favorable conditions. More work can be done in different atmospheric environments

This analysis provides future researchers with expectations of how CO_2 concentrations should look in the PBL and the free troposphere and how that atmosphere can affect the vertical structure. By analyzing the structure of CO_2 in heavily populated and heavily vegetated areas, we could generalize these findings to other surface types.

Acknowledgments. The corresponding author would like to thank the National Weather Center Research Experience for Undergraduates (NWC REU) for providing the opportunity to conduct this research. I would also like to thank Melanie Schroers and Jacqueline Waters as well as the other NWC REU students for support and guidance through this experience. The corresponding author would also like to thank the Geostationary Carbon Cycle Observatory for providing a comfortable workspace.

This material is based upon work supported by the National Science Foundation under Grant No. AGS-1560419.

References

Fischer, J., and D. B. Lindenmayer, 2007: Landscape modification and habitat fragmentation: a synthesis. *Global Ecology and Biogeography*, **16 (3)**.

Friedlingstein, P., M. Meinshausen, V. K. Arora, C. D. Jones, A. Anav, S. K. Liddicoat, and R. Knutti, 2014: Uncertainties in cmip5 climate projections due to carbon cycle feedbacks. *Journal of Climate*, **27 (2)**, 511–526, doi:10.1175/JCLI-D-12-00579.1, URL https://doi.org/10.1175/JCLI-D-12-00579.1.

Friedlingstein, P., and Coauthors, 2006: Climatecarbon cycle feedback analysis: Results from the c4mip model intercomparison. *Journal of Climate*, **19 (14)**, 3337–3353, doi:10.1175/JCLI3800.1.

Helliker, B. R., and Coauthors, 2004: Estimates of net co2 flux by application of equilibrium boundary layer concepts to co2 and water vapor measurements from a tall tower. *Journal of Geophysical Research: Atmospheres*, **109 (D20)**.

Hilton, T. W., K. J. Davis, and K. Keller, 2014: Evaluating terrestrial co_2 flux diagnoses and uncertainties from a simple land surface model and its residuals. *Biogeosciences*, **11 (2)**, 217–235, doi:10.5194/bg-11-217-2014, URL https://www.biogeosciences.net/11/217/2014/.

Hilton, T. W., K. J. Davis, K. Keller, and N. M. Urban, 2013: Improving north american terrestrial co_2 flux diagnosis using spatial structure in land surface model residuals. *Biogeosciences*, **10 (7)**, 4607–4625, doi:10.5194/bg-10-4607-2013, URL https://www.biogeosciences.net/10/4607/2013/.

Hu, X.-M., S. Crowell, and Q. Wang, 2018a: Co2 dynamical downscaling in 2016 over the contiguous united states using wrf-vprm, a weather-biosphere-online-coupled model. to be submitted. *Journal of Geophysical Research*, **109 (D20)**.

Hu, X.-M., Y. Zhang, S. Crowell, M. Xue, B. Moore, X. Xiao, . . ., and K. J. Davis, 2018: .

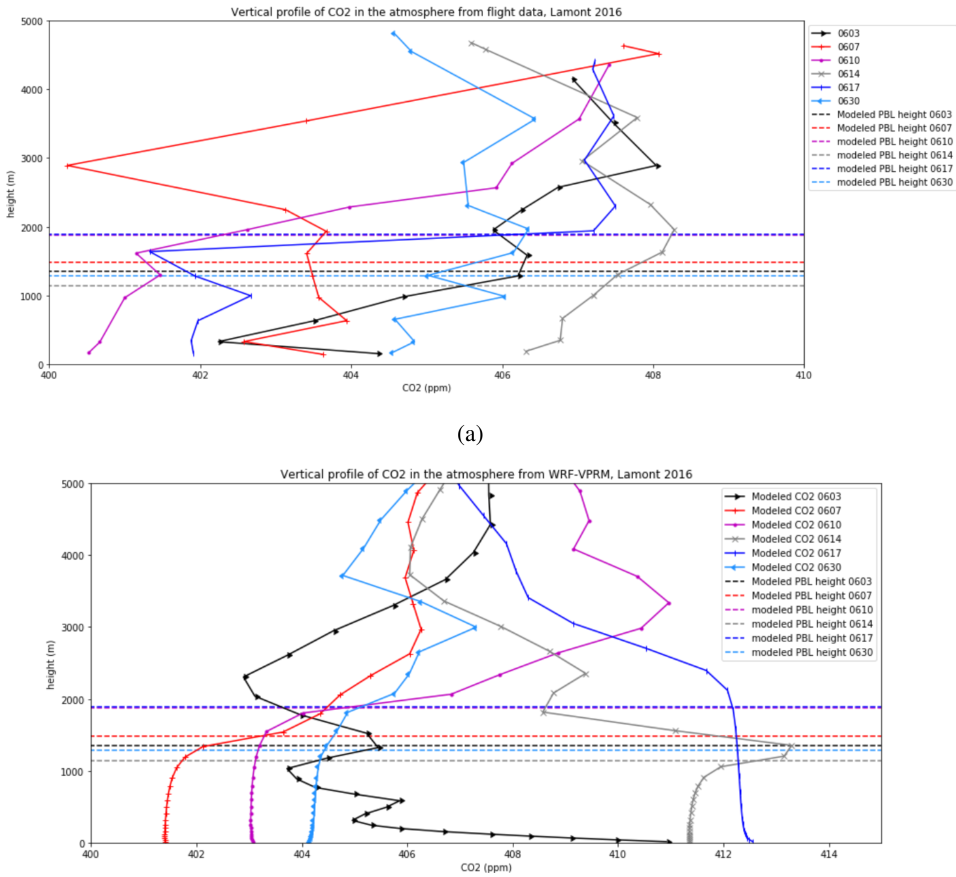

FIG. 6: Vertical profile of CO_2 concentration collected during flights of June 2016 with modeled PBL depths (a) and modeled vertical profile of CO_2 with modeled PBL depth (b).

Huete, A., K. Didan, T. Miura, E. Rodriguez, X. Gao, and L. Ferreira, 2002: Overview of the radiometric and biophysical performance of the modis vegetation indices. *Remote Sensing of Environment*, **83 (1)**, 195 – 213, doi:https://doi.org/10.1016/S0034-4257(02)00096-2, URL http://www.sciencedirect.com/science/article/pii/S0034425702000962, the Moderate Resolution Imaging Spectroradiometer (MODIS): a new generation of Land Surface Monitoring.

Lan, X., and Coauthors, 2017: Gradients of column co_2 across north america from the noaa global greenhouse gas reference network. *Atmospheric Chemistry and Physics*, **17 (24)**, 15 151–15 165, doi:10.5194/acp-17-15151-2017, URL https://www.atmos-chem-phys.net/17/15151/2017/.

Panofsky, H., 1985: The planetary boundary layer. *Advances in Geophysics*, **28**, 359–385.

United States Census, cited 2018: American Fact Finder. [Available online at https://factfinder.census.gov/faces/nav/jsf/pages/index.xhtml].

Yi, C., K. J. Davis, P. S. Bakwin, A. S. Denning, G. N. Zhan, A. Desai, J. C. Lin, and C. Gerbig, 2004: Observed covariance between ecosystem carbon exchange and atmospheric boundary layer dynamics at a site in northern wisconsin. *Journal of Geophysical Research: Atmospheres*, **109**.

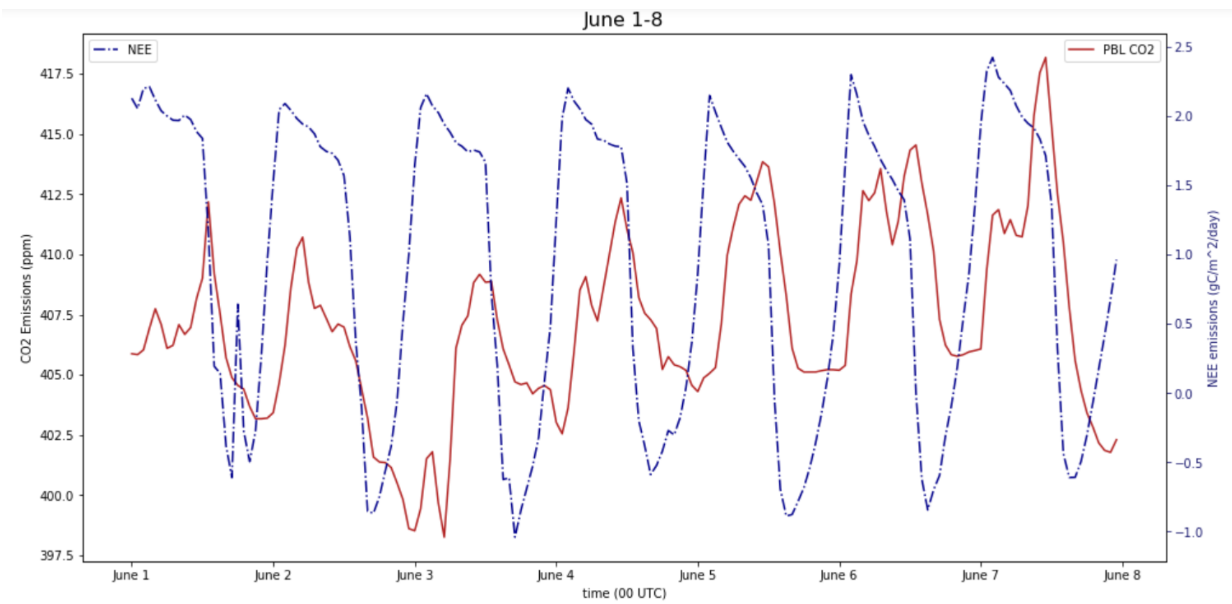

FIG. 7: NEE and PBL CO_2 over a weekly timescale, June 1-8

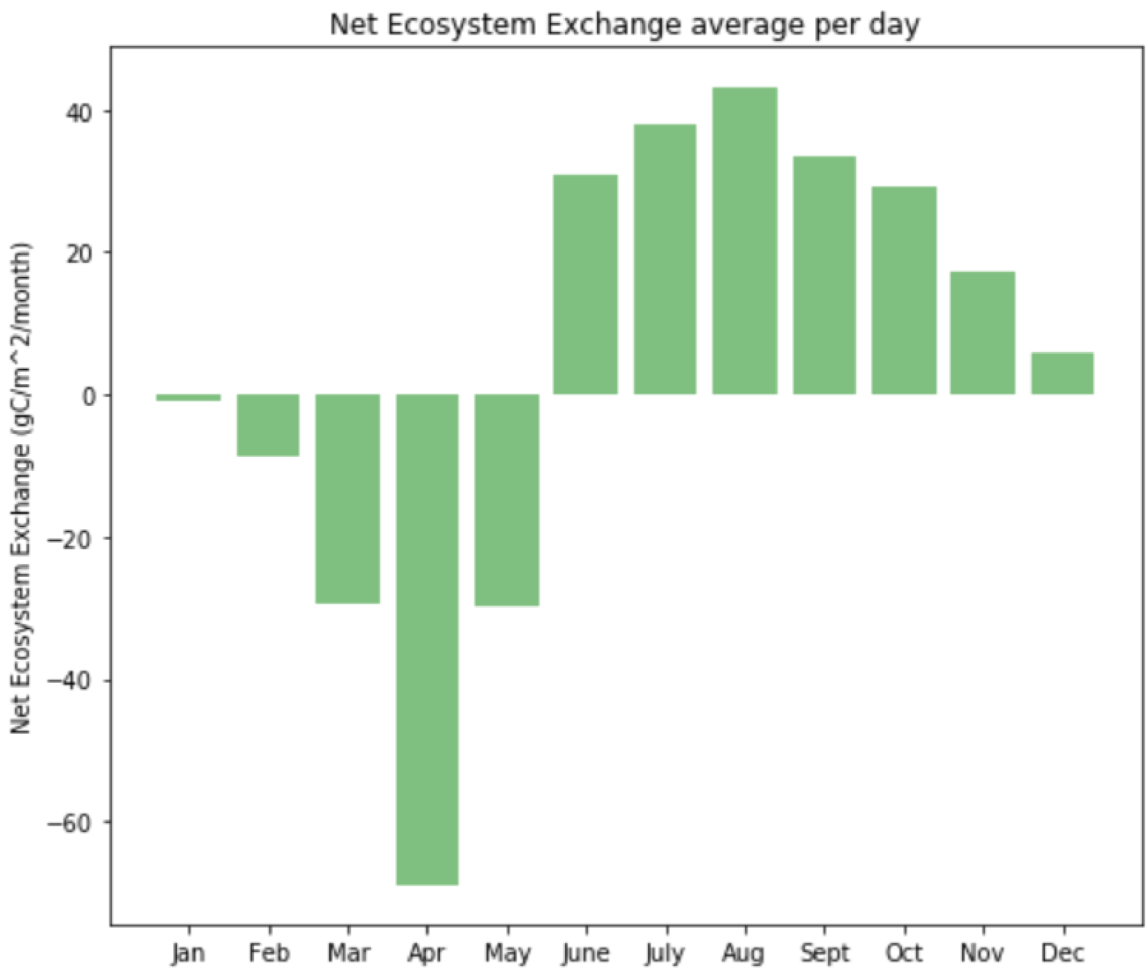

FIG. 8: Average daily NEE flux per month modeled by WRF-VPRM.

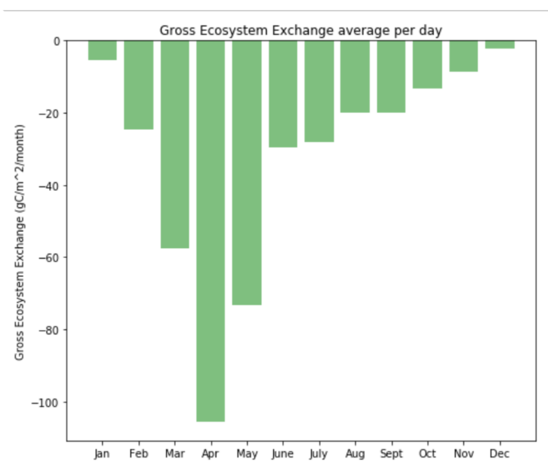

(a) Average daily GEE flux per month modeled by WRF-VPRM.

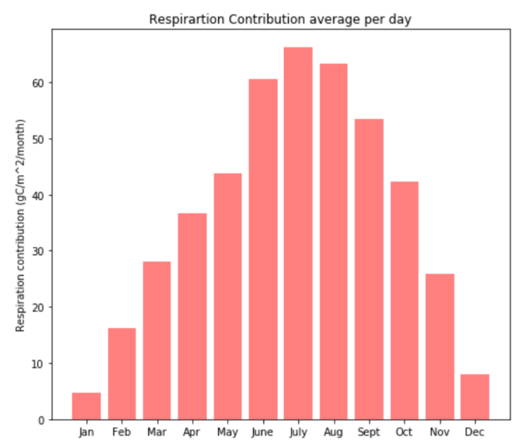

(b) Average daily respiration flux per month modeled by WRF-VPRM.

FIG. 9: Comparisons of GEE and respiration components of NEE.